Atomistic mechanisms for bilayer growth of graphene on metal substrates

Wei Chen, Ping Cui, Wenguang Zhu, Efthimios Kaxiras, Yanfei Gao, and Zhenyu Zhang

Phys. Rev. B **91**, 045408 — Published 8 January 2015

DOI: 10.1103/PhysRevB.91.045408

Atomistic mechanisms for bilayer growth of graphene on metal substrates

Wei Chen,[1,2,3] Ping Cui,[1] Wenguang Zhu,[1] Efthimios Kaxiras,[3] Yanfei Gao,[2,4] and Zhenyu Zhang[1]

[1] *International Center for Quantum Design of Functional Materials (ICQD), Hefei National Laboratory for Physical Sciences at Microscale, and Synergetic Innovation Center of Quantum Information and Quantum Physics, University of Science and Technology of China, Hefei, Anhui 230026, China*

[2] *Department of Materials Science and Engineering, University of Tennessee, Knoxville, Tennessee 37996, USA*

[3] *Department of Physics, Harvard University, Cambridge, Massachusetts 02138, USA*

[4] *Materials Science and Technology Division, Oak Ridge National Laboratory, Oak Ridge, Tennessee 37831, USA*

(Dated: November 24, 2014)

Epitaxial growth on metal substrates has been shown to be the most powerful approach in producing large-scale high-quality monolayer graphene, yet it remains a major challenge to realize uniform bilayer graphene growth. Here we carry out a comparative study of the atomistic mechanisms for bilayer graphene growth on the (111) surfaces of Cu and Ni, using multi-scale approaches combining first-principles calculations and rate equation analysis. We first show that the relatively weak graphene-Cu interaction enhances the lateral diffusion and effective nucleation of C atoms underneath the graphene island, thereby making it more feasible to grow bilayer graphene on Cu. In contrast, the stronger graphene-Ni interaction suppresses the lateral mobility and dimerization of C atoms underneath the graphene, making it unlikely to achieve controlled growth of bilayer graphene on Ni. We then determine the critical graphene size beyond which nucleation of the second layer will take place. Intriguingly, the critical size exhibits an effective inverse "Ehrlich-Schwoebel barrier" effect, becoming smaller for faster C migration from the Cu surface to the graphene-Cu interface sites across the graphene edge. These findings allow us to propose a novel alternating growth scheme to realize mass production of bilayer graphene.

PACS numbers: 81.05.ue, 81.15.Aa, 68.55.A-, 68.43.Bc

I. INTRODUCTION

Graphene, the one-atom-thick carbon nanosheet has drawn tremendous research attention since its first experimental achievement by mechanical cleavage methods.[1,2] Pristine monolayer graphene is a semimetal with zero band gap, which severely impedes its potential applications in logic devices.[3] To overcome this inherent issue, bilayer graphene has been exploited to have a tunable gap with an external electric field,[4,5] making it highly desirable to achieve large-scale single-crystalline graphene bilayers for a variety of fundamental and technological reasons.

It has been established experimentally that epitaxial growth on transition metal substrates, especially on Cu and Ni, is one of the most appealing approaches in graphene production.[6,7] Subsequent theoretical studies of the atomistic growth mechanisms have emphasized the importance of fast diffusion and effective nucleation of the C adatoms in facilitating high-quality growth of graphene on Cu.[8] However, largely because of the low catalytic reactivity for dehydrogenation on top of graphene and low C solubility inside Cu, graphene growth on Cu substrates is predominantly monolayer, in contrast to the typical multilayer but uncontrollable graphene growth on Ni substrates via efficient segregation and precipitation of highly soluble C atoms.[9] Extensive experimental efforts have also been made to increase the graphene thickness on Cu,[10–15] but hitherto only with limited success. To overcome this standing challenge, several new approaches have been proposed based on first-principles studies of graphene bilayer growth on Cu.[16,17] In particular, it has been proposed that effective H passivation of the edge sites of the growing first monolayer may significantly enhance the growth rate of the second layer underneath.[16] However, a comprehensive study accessing the delicate competitions between the various atomistic processes involved in nonequilibrium growth of graphene bilayers on different metal substrates is still critically needed, in order to define the physically realistic conditions for eventual experimental realization of mass production of high-quality bilayer graphene.

In this article, we carry out a comparative and comprehensive study of the atomistic processes and their delicate competitions in bilayer graphene growth on the (111) surfaces of Cu and Ni, using multi-scale approaches combining first-principles calculations and rate equation analysis. We focus on Cu and Ni in the present study because of the following considerations: First, Cu and Ni are inexpensive and highly catalytic metal substrates. Secondly and more importantly, graphene grown on Cu and Ni is large-scale, high-quality, and easily transferable to other substrates for characterization and potential device applications.[6,7,9] We expect that the underlying atomistic mechanisms for graphene bilayer growth revealed on these two substrates may also find relevance in graphene growth on other catalytic metal substrates.[18–20] Here we first show that the relatively weak graphene-Cu interaction enhances the lateral diffusion and effective nucleation of C atoms underneath the graphene island,

thereby making it more feasible to grow bilayer graphene on Cu. In contrast, the stronger graphene-Ni interaction suppresses the lateral mobility and dimerization of C atoms underneath the graphene, making it less likely to achieve controlled growth of bilayer graphene on Ni. We then determine the critical graphene size beyond which nucleation of the second layer will take place. Intriguingly, the critical size exhibits an effective inverse Ehrlich-Schwoebel (ES) barrier[21,22] effect, becoming smaller for faster C migration from the Cu surface to the graphene-Cu interface sites across the graphene edge. The new insights gained in the present study also allow us to propose a novel alternating growth scheme to realize mass production of bilayer graphene. These findings may prove instrumental in eventual realization of mass production of high-quality bilayer graphene for device applications.

The article is organized as follows: In Section II, we present our studies of the atomistic processes in bilayer graphene growth on Cu(111) and Ni(111) using first-principles calculations. The results clearly favor Cu to be the substrate of choice for growing bilayer graphene. In Section III, we develop a rate equation description to analyze the critical graphene size, beyond which nucleation of the second layer will take place. The dependence of the second-layer growth on different physical conditions is also included. In Section IV, we discuss the possible strategy for optimizing bilayer graphene growth on Cu, and reveal the potential existence of an intriguing effective inverse ES barrier effect in such bilayer growth. Finally, we summarize our results in Section V.

II. FIRST-PRINCIPLES CALCULATIONS

In the first-principles part of our studies, we perform density functional theory (DFT) calculations using the Vienna *ab initio* simulation package (VASP),[23] with projector-augmented wave (PAW) potentials[24,25] and the generalized gradient approximation (GGA-PBE)[26] for the exchange-correlation function. DFT-D2,[27,28] a semi-empirical approach is used to include the van der Waals (vdW) interactions. The lattice constants of metals are obtained via structural optimization. The metal (111) surfaces are modeled by slabs of five atomic layers, and the graphene-metal systems are modeled by placing a graphene overlay on top of the metal surfaces. The vacuum layers are thick enough to ensure decoupling between neighboring slabs. During relaxation, atoms in the lower two atomic layers are fixed in their respective bulk positions, and all the other atoms are allowed to relax. A 3×3×1 k-point mesh is used for the 3×3 surface unit cell of metals,[29] similar to the setup in the previous studies of Ni systems.[30,31] In the present study, all the calculations are spin-polarized, with the atoms in the supercells all initiated with finite magnetic moments. After structural relaxation and energy convergence, Cu becomes nonmagnetic, Ni is ferromagnetic, and an isolated C atom preserves its finite magnetic moment. We note

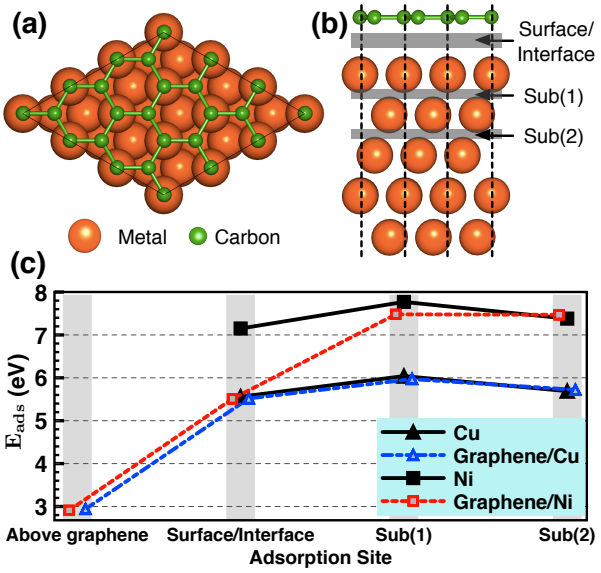

FIG. 1: (Color online). (a) Top and (b) side views of monolayer graphene adsorbed on a metal substrate. The bare surface or graphene/metal interface sites, as well as the first and second subsurface sites (Sub(1) and Sub(2)) are also indicated. (c) The carbon adsorption energies at different sites. We slightly shift the curves of graphene/Cu and graphene/Ni horizontally for clarity purpose.

that the inherent magnetic aspect of the Ni substrate may affect the diffusion of the spin-polarized C adatom, and such effects are properly accounted for. We use the climbing image nudged elastic band (CI-NEB) method[32] to determine the potential energy barriers of the various carbon diffusion processes, with three to five intermediate images constructed along each pathway.

To investigate the growth mechanisms of bilayer graphene, we first model the interfaces of a single-layer graphene adsorbed on Cu(111) and Ni(111) surfaces. To account for the small lattice mismatch between graphene and Cu(111) or Ni(111),[33–36] we use 3×3 graphene supercells, whose lattice constants have been slightly stretched to match those of the metal supercells, an approach commonly used in previous studies.[17,37,38] As illustrated in Figs. 1a and 1b, the graphene overlayer prefers to stay on these surfaces with half of the carbon atoms directly above the topmost metal atoms, and the other half at the fcc hollow sites. The spacing between graphene and the substrate is 2.91 Å on Cu, and is 2.08 Å on Ni, consistent with experimental results.[39] The DFT-D2 method thus well describes the contrasting features of graphene bonding with Cu (*weak*) and Ni (*strong*).

Given the interfacial structures, we then explore the behaviors of various carbon sources at the graphene-metal interfaces. It has been speculated recently that hydrogenated carbon molecules may diffuse into the interfacial region through the graphene edge.[14] But such a scenario is unlikely, based on the recent observations

that the bare graphene edge usually forms strong bonding with the catalytic metal substrates,[16,40–43] leaving very limited space for the molecules to across the edge sites. Furthermore, our present study shows that the presence of any of the hydrogenated carbon source molecules (CH_n, with n = 1, 2, 3, or 4) at the interface will substantially enlarge the graphene-Cu spacing to more than 4.25 Å at high energy costs. In contrast, a single C atom underneath the graphene is still energetically favorable and also barely changes the graphene-Cu interfacial distance. Therefore, we focus on the behaviors of C adatoms hereafter in studying bilayer growth.

As indicated in Fig. 1b, we first consider the energetics of several different carbon adsorption sites: on the bare metal substrate, on the top of the graphene, between the graphene and metal, and in the first and second subsurface layers of the metal substrate. The explored surface or interface positions include fcc hollow, hcp hollow, bridge, and top sites, and for the subsurface layers, we consider both tetrahedral and octahedral sites. The corresponding adsorption energies, defined as $E_{ads} = E_C + (E_{metal}$ or $E_{graphene/metal}) - E_{total}$, are summarized in Fig. 1c. A large E_{ads} indicates a large reduction of energy upon adsorption and hence a stable state. The results indicate that the top of the graphene is the least favorable adsorption site for either Cu or Ni, implying that the second-layer graphene should grow below the existing graphene layer.[13,14] Similar to the bare substrate case, the first subsurface site remains the most favorable in the presence of the graphene overlayer on both substrates, with minimal changes in the C adsorption energies.

We now investigate C adatom diffusion within and between the different regions, including five major diffusion pathways, as illustrated in Fig. 2. The energy of the C adatom adsorbed on the surface or at the interface is set to 0 as the reference, with the potential barrier heights for the different diffusion paths indicated explicitly. Our results show that, on the Cu substrate underneath the graphene overlayer, the C diffusion barrier between the first subsurface sites is 0.33 eV, reduced by 0.22 eV from that on the bare Cu substrate, consistent with the findings in a recent study.[16] In contrast, the diffusion barrier at the graphene-Cu interface is substantially enlarged by 0.48 eV from that on the bare surface. More importantly, since the first subsurface sites are more stable than the interface sites by $\sim$ 0.5 eV, hopping between the first subsurface sites should be the major route for C lateral diffusion during the second-layer graphene growth on the Cu substrate. In comparison, the energetic and kinetic processes on Ni exhibit distinct differences. First, the energy difference for C adsorption at the subsurface sites relative to the surface sites is enlarged by $\sim$ 1.3 eV in the presence of the graphene overlayer, consistent with the expectation of high C solubility in Ni. In addition, the C diffusion barriers between the subsurface sites are much higher than those on the Cu substrate, either in the absence or presence of the graphene overlayer. Collectively, these results show that the Cu substrate offers much higher C lateral mobility underneath the graphene overlayer than the Ni substrate, a distinctly important aspect for bilayer graphene growth.

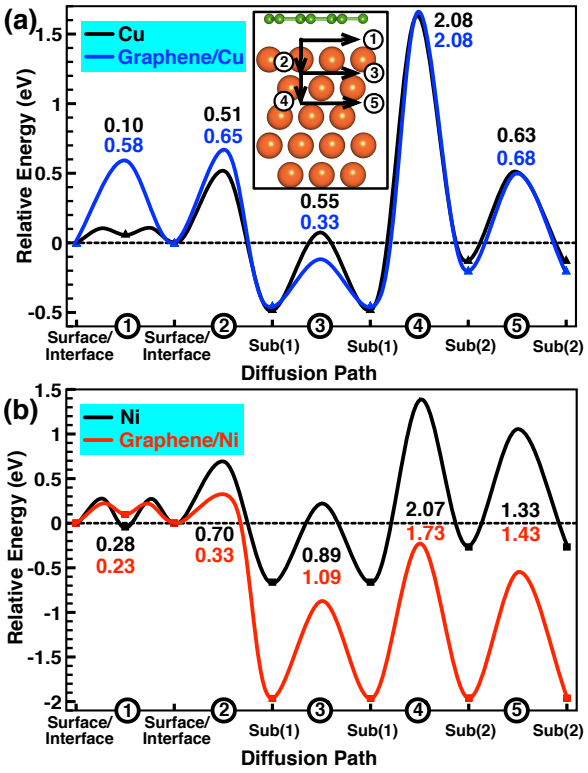

FIG. 2: (Color online). Minimum energy paths of carbon diffusion within and between the different regions indicated in Figure 1 on (a) Cu and (b) Ni. The numbers in the horizontal axes correspond to the routes shown in the inset of (a).

We next examine the carbon dimerization processes in the presence of the graphene overlayer. Beyond the previous consideration on the Cu and Ni surfaces,[8] here we also take subsurface sites into account. In our calculations, we place two carbon atoms at the surface/interface or first subsurface sites, then increase their distance to perform structural relaxation, and investigate the total energy versus distance between the two C atoms. In these processes, we have checked all the possible C adsorption sites at the surface/interface and first subsurface layers, and for each C-C configuration spin polarization is specifically considered. Our results suggest that, on the Cu substrate, the two C atoms always prefer to form a dimer either at the interface or subsurface sites. In contrast, two such carbon atoms always prefer to stay apart in the subsurface or bulk sites of Ni, but show slight preference of dimerization if they are limited to the interface sites. Therefore, the critical size for nucleation and growth of a second-layer graphene underneath the first layer is expected to be much smaller on Cu than that on Ni. Indeed, the uncontrollable multilayer growth on Ni sub-

strates requires much higher solubility of C atoms inside the bulk, and efficient precipitation of such C atoms towards the surface at substantially reduced temperatures. In contrast, bilayer growth on Cu has been shown to be initiated at high growth temperatures and insignificant carbon solubility in the bulk.

III. RATE EQUATION ANALYSIS

So far we have limited ourselves to qualitative discussions based on the energetics and kinetics from first-principles calculations. Next we develop a rate equation description to gain more insights on the delicate competitions between the various rate processes, and potentially define the physical conditions for optimizing bilayer growth on Cu. To capture the essential physics without losing generality, we consider a simplified model consisting of an existing circular-shaped graphene island with radius R on a Cu substrate (see Fig. 3a). Active C adatoms may diffuse across or attach to the edge of the graphene island from the bare terrace sites or sites underneath the graphene; the corresponding rates are given by $D_0\exp(-V_i/kT)$, where V_i refers to the activation barrier against the diffusion process i, D_0 is the attempt frequency, k is the Boltzmann constant, and T is the growth temperature. We define the density of C adatoms on the bare substrate as η_{ext} and that under the graphene island as η_{int}, given by the number of C adatoms per adsorption site in the area of a^2, respectively. Since the growth system is typically kept at a constant pressure of hydrocarbon gas and a constant growth temperature, η_{ext} can be approximated by a constant when a sizable first-layer graphene has been formed. In contrast, η_{int} is expected to monotonically increase to a steady value at a later stage of the growth.

Because the amount of C adatoms active for diffusion across or attachment to the graphene edge is proportional to the C adatom density and the perimeter of the boundary, the growth rate of the first-layer graphene can be written as:

$$\frac{d[\pi R^2(t)]}{a^2\cdot dt} = c\cdot[\eta_{ext}+\eta_{int}(t)]\,2\pi R(t)\cdot\frac{1}{\alpha+1}, \qquad (1)$$

where c is a proportional coefficient,

$$\alpha = \exp[-(V_{ac}-V_{at})/kT] \qquad (2)$$

is the ratio of the C adatom diffusion rate across the boundary (barrier V_{ac}) over the attachment rate at the graphene edge (barrier V_{at}). Since the presence of the graphene overlayer barely changes the C adsorption energies (see Fig. 1c), C adatom diffusion into and out of the region under the first layer encounters essentially the same effective barrier.

Per unit time, because the number of the C adatoms going through the graphene edge and the increased area of the first layer are both proportional to R, we can expect the steady state value of $\eta_{int}(r,\ t)$ to be only weakly dependent on r: $\eta_{int}(r,\ t) = \eta_{int}(t)$ $(r < R)$. Accordingly, the change of the total amount of the C adatoms underneath the first layer can be written as:

$$\frac{d[\eta_{int}(t)\,\pi R^2(t)]}{a^2\cdot dt} = c\cdot[\eta_{ext}-\eta_{int}(t)]\,2\pi R(t)\cdot\frac{\alpha}{\alpha+1}. \qquad (3)$$

Dividing Eq.(1) by Eq.(3), we obtain:

$$R\,\frac{d\eta_{int}}{dR} = 2\,(\frac{\eta_{ext}-\eta_{int}}{\eta_{ext}+\eta_{int}}\cdot\alpha-\eta_{int}). \qquad (4)$$

Solving Eq.(4) for the system in the steady state, we obtain a simple expression for the adatom density underneath the graphene as:

$$\eta_{int} = \frac{1}{2}\left[\sqrt{\eta_{ext}^2+\alpha^2+6\,\eta_{ext}\,\alpha}-(\eta_{ext}+\alpha)\right]. \qquad (5)$$

From Eq.(5) we see that η_{int} is determined by three important physical factors: the extra barrier $V_{ac}-V_{at} = V_{ES}$, which is equivalent to the ES barrier in the traditional field of thin film growth;[21,22] η_{ext}, which sensitively depends on the pressure of the hydrocarbon source; and the substrate temperature T. Whereas the first factor reflects the intrinsic properties of the system and can be potentially tuned by, e.g., H passivation of the edge sites,[16] the latter two factors can be more readily controlled in a specific growth experiment.

For quantitative estimates, we choose a typical growth temperature of $T = 1300$ K, and plot the dependence

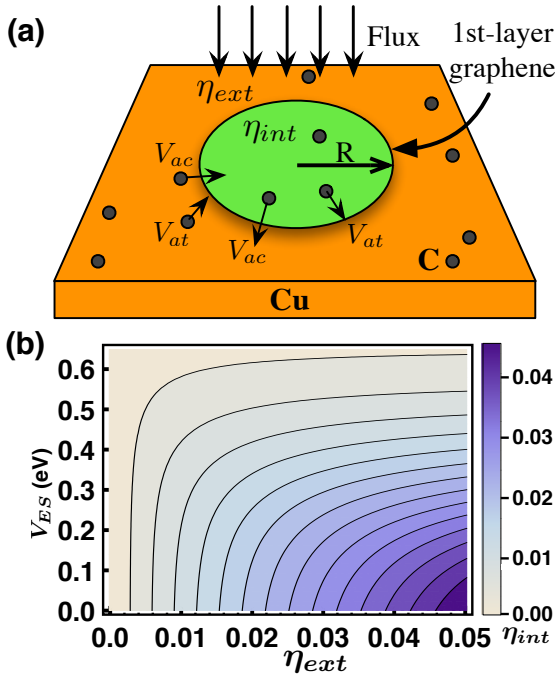

FIG. 3: (Color online). (a) Schematic illustration of the competing rate processes in bilayer graphene growth on Cu. (b) Dependence of adatom density η_{int} on η_{ext} and V_{ES} at $T =$ 1300 K.

of η_{int} on η_{ext} and V_{ES} in Fig. 3b. As seen clearly, to maximize η_{int}, higher hydrocarbon gas pressure for large η_{ext} and lower V_{ES} are needed. At relatively small V_{ES} and large η_{ext}, η_{int} depends sensitively on both parameters. However, once V_{ES} is larger than ~ 0.5 eV, or η_{ext} is smaller than ~ 0.01, η_{int} becomes very tiny, regardless of the other parameter. Meanwhile, even though it is not explicitly shown in Fig. 3b, high temperatures are clearly also helpful to achieve sufficiently high η_{int} for second-layer graphene growth. This last observation is consistent with the experiments.[14]

Next, we investigate the nucleation rate of the second-layer graphene island, which can be expressed as: $\omega = \gamma a^{-4} D \eta_{int}^{\nu}$,[44] where D is the diffusion coefficient, and ν is the number of C atoms in the smallest compact islands that can stably exist. D depends on the diffusion barrier (V_{d_2}) underneath the first layer: $D = D_0 \exp(-V_{d_2}/kT)$, where D_0 typically lies between 10^{-2} and 10^{-3} cm^{2}s^{-1}.[45] We further have $\gamma = \sigma_\nu \exp(E_v/kT)$, where σ_ν is the capture number (within the range of 2 - 4 as an approximation),[46] and E_v is the energy difference between a compact island and a linear chain, both with ν carbon atoms. The rate that a compact island nucleates under the first-layer graphene then can be determined as: $\Omega = \int_0^R \omega 2\pi r \, dr = \omega \pi R^2$.[44]

The probability of the first-layer island to have a new island nucleated underneath is then $f = 1 - \exp(-\Omega t)$.[44] Since $\Omega \propto R^2$ and $R \propto t$, we have:

$$f = 1 - \exp[-(R/R')^3], \tag{6}$$

where

$$R' = \left[\frac{(\eta_{ext} + \eta_{int})\, c\, a^6}{\gamma D \eta_{int}^{\nu} \pi\, (1+\alpha)} \right]^{\frac{1}{3}}. \tag{7}$$

As shown in Fig. 4a, f increases rapidly when R is close to R'. By defining a critical radius R_c at which the nucleation probability f is 0.5, we have:

$$R_c = (\ln 2)^{\frac{1}{3}} R' \sim 0.88\, R'. \tag{8}$$

Indeed, $f(R/R')$ has the highest slope at $R = (\frac{2}{3})^{\frac{1}{3}} R' \sim 0.87\, R'$, close to R_c.

The dependence of the critical size R_c on the extra edge crossing barrier V_{ES} at different growth temperatures is shown in Fig. 4b. Here we have chosen physically realistic values of $\frac{dR}{dt} = 1\mu$m/min[47] to estimate the proportional constant c in Eq.(1), and $\eta_{ext} = 0.03, a \sim 10^{-10}$ m, $D_0 = 10^{-6}$ m^2 s^{-1}, $V_{d_2} = 0.33$ eV, $\sigma_\nu = 3$, $\nu = 10$, and $E_v \sim -1.5$ eV.[48] The downward shift of the curves indicates that the critical size R_c decreases as the temperature T increases.

To make closer connection with experiments, we note that a recent study reported $V_{ES} = 0.53$ eV (Figs. 5a and 6a in Ref. 16) at the bare graphene edge without H passivation. From Fig. 4b, the corresponding R_c is on the order of tens of *micrometres* at $T = 1300$ K, which explains the experimental observation that at typical

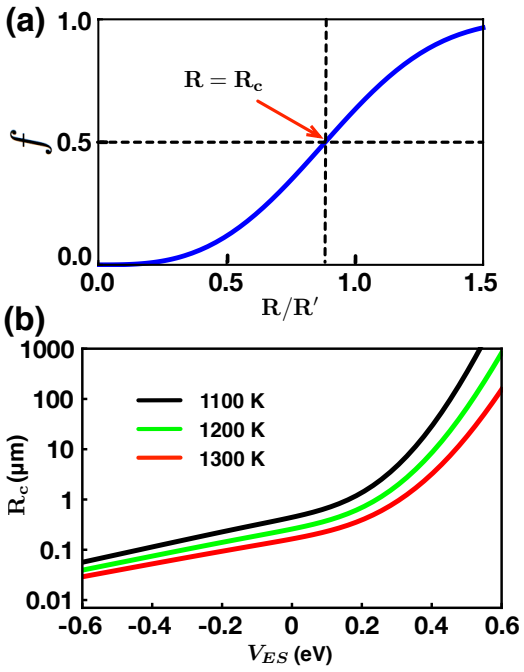

FIG. 4: (Color online). (a) Nucleation probability $f(R/R')$, with the critical radius of the first-layer graphene indicated by R_c. (b) Dependence of R_c on V_{ES} at different growth temperatures.

growth conditions with low H_2 concentrations, second-layer graphene is suppressed.[6] It is therefore necessary to find efficient ways to lower V_{ES} in order to promote bilayer graphene growth.

In this regard, we note that V_{ac} and V_{at} can be reduced and enlarged with H passivation on the graphene edge to 0.84 eV and 1.67 eV from their original values of 1.15 eV and 0.62 eV, respectively.[16] In an actual growth process, graphene edge is more likely to be partially saturated by H. The passivated periphery offers fast channels for C adatoms to cross the boundary, while the unpassivated sites sustain the growth of the first layer. With increasing H_2 pressure, V_{ES} can be effectively further reduced. For the case that half of the graphene edge sites are passivated by H, we can estimate R_c to be on the order of several hundred *nanometers*, which roughly represents the success of the experimental efforts to date in growing bilayer graphene using higher H_2 pressure.[14] In the more desirable situation that most of the edge sites of the first layer are properly passivated, V_{ES} can become negative, effectively suppressing the enlargement of the first layer, and also leading to further reduced R_c down to the range of tens of *nanometers* (Fig. 4b).

IV. DISCUSSIONS

The above analysis suggests that tuning the hydrogen pressure can be an effective approach to change the relative ratio of the growth rates of the two layers. To fabricate large-scale uniform bilayer graphene, here we propose an alternating growth strategy: switching on or off the hydrogen pressure between two extreme situations. At very low hydrogen pressure, only the first-layer graphene grows predominantly; while at very high hydrogen pressure, only the second-layer graphene enlarges predominantly. Growth of the first layer should be turned on once the second layer reaches comparable sizes. In addition, the decoration of graphene edge to reduce V_{ES} is not necessarily limited to hydrogen passivation; other elements or molecules are also worth exploring to further alter the growth rate of the adlayer graphene, which should be addressed in a future study.

Before closing, it is interesting to note that, here we have demonstrated a growth picture that is opposite to the conventional multilayer growth,[44,49–51] where larger additional diffusion barriers at the step edge (ES barrier[21,22]) lead to higher nucleation probabilities of the second-layer islands. In contrast, here the higher the V_{ES}, the lower the growth rate of the second layer underneath. Therefore, V_{ES} can be viewed as an effective *inverse* ES barrier, even though its sign is still positive. This intriguing aspect should also be applicable to other multilayer growth systems where the second layer grows from underneath and acquires atom supplies from the boundary of the first layer.

V. CONCLUSIONS

In summary, we have provided a comparative and comprehensive study of the atomistic mechanisms in bilayer graphene growth on the (111) surfaces of Cu and Ni, using multi-scale approaches combining first-principles calculations and rate equation analysis. Our studies clearly favor Cu to be the substrate of choice for growing bilayer graphene. We have also determined the critical graphene size beyond which nucleation of the second layer will take place, and proposed an alternating growth scheme for controlled fabrication of large-scale uniform bilayer graphene. The present study further revealed the potential existence of an intriguing effective inverse ES barrier effect in such bilayer (and multilayer) growth, where the growth of the subsequent layers proceeds underneath the first layer.

ACKNOWLEDGMENTS

We are grateful to Hua Chen and Ekin D. Cubuk for helpful discussions. This work was supported by the National Natural Science Foundation of China (Grant Nos. 11034006, 11204286, and 11374273), the National Key Basic Research Program of China (Grant No. 2014CB921103), the U.S. National Science Foundation (Grant Nos. DMR 1206960 and CMMI 1300223), and the U.S. Department of Energy (Grant No. DE-FG03-02ER45958). The calculations were performed at National Energy Research Scientific Computing Center (NERSC) of the U.S. Department of Energy.

[1] K. S. Novoselov, A. K. Geim, S. V. Morozov, D. Jiang, Y. Zhang, S. V. Dubonos, I. V. Grigorieva, and A. A. Firsov, Science **306**, 666 (2004).
[2] A. K. Geim, Science **324**, 1530 (2009).
[3] A. H. Castro Neto, F. Guinea, N. M. R. Peres, K. S. Novoselov, and A. K. Geim, Rev. Mod. Phys. **81**, 109 (2009).
[4] Y. B. Zhang, T. Tang, C. Girit, Z. Hao, M. C. Martin, A. Zettl, M. F. Crommie, Y. R. Shen, and F. Wang, Nature **459**, 820 (2009).
[5] A. N. Pal and A. Ghosh, Appl. Phys. Lett. **95**, 082105 (2009).
[6] X. S. Li *et al.*, Science **324**, 1312 (2009).
[7] K. S. Kim, Y. Zhao, H. Jang, S. Y. Lee, J. M. Kim, K. S. Kim, J.-H. Ahn, P. Kim, J.-Y. Choi, and B. H. Hong, Nature **457**, 706 (2009).
[8] H. Chen, W. G. Zhu, and Z. Y. Zhang, Phys. Rev. Lett. **104**, 186101 (2010).
[9] X. S. Li, W. W. Cai, L. Colombo, and R. S. Ruoff, Nano Lett. **9**, 4268 (2009).
[10] S. Lee, K. Lee, and Z. H. Zhong, Nano Lett. **10**, 4702 (2010).
[11] K. Yan, H. L. Peng, Y. Zhou, H. Li, and Z. F. Liu, Nano Lett. **11**, 1106 (2011).
[12] M. Kalbac, O. Frank, and L. Kavan, Carbon **50**, 3682 (2012).
[13] S. Nie, W. Wu, S. R. Xing, Q. K. Yu, J. M. Bao, S. Pei, and K. F. McCarty, New J. Phys. **14**, 093028 (2012).
[14] Q. Y. Li *et al.*, Nano Lett. **13**, 486 (2013).
[15] W. Song *et al.*, Carbon **68**, 87 (2014).
[16] X. Y. Zhang, L. Wang, J. Xin, B. I. Yakobson, and F. Ding, J. Am. Chem. Soc. **136**, 3040 (2014).
[17] P. Wu, X. F. Zhai, Z. Y. Li, and J. L. Yang, J. Phys. Chem. C **118**, 6201 (2014).
[18] P. W. Sutter, J.-I. Flege, and E. A. Sutter, Nat. Mater. **7**, 406 (2008).
[19] J. Coraux *et al.*, New J. Phys. **11**, 023006 (2009).
[20] T. Oznuluer, E. Pince, E. O. Polat, O. Balci, O. Salihoglu, and C. Kocabas, Appl. Phys. Lett. **98**, 183101 (2011).
[21] G. Ehrlich and F. G. Hudda, J. Chem. Phys. **44**, 1039 (1966).
[22] R. L. Schwoebel, J. Appl. Phys. **40**, 614 (1969).
[23] G. Kresse and J. Furthmüller, Phys. Rev. B **54**, 11169 (1996).
[24] P. E. Blöchl, Phys. Rev. B **50**, 17953 (1994).
[25] G. Kresse and D. Joubert, Phys. Rev. B **59**, 1758 (1999).
[26] J. P. Perdew, K. Burke, and M. Ernzerhof, Phys. Rev. Lett. **77**, 3865 (1996).
[27] S. Grimme, J. Comput. Chem. **27**, 1787 (2006).
[28] T. Bučko, J. Hafner, S. Lebègue, and J. G. Ángyán, J.

Phys. Chem. A **114**, 11814 (2010).
[29] M. Methfessel and A. T. Paxton, Phys. Rev. B **40**, 3616 (1989).
[30] F. Abild-Pedersen, J. K. Nørskov, J. R. Rostrup-Nielsen, J. Sehested, and S. Helveg, Phys. Rev. B **73**, 115419 (2006).
[31] Y. Zhu, Y. Dai, D. Chen, and W. Yuan, Surf. Sci. **601**, 1319 (2007).
[32] G. Henkelman, B. P. Uberuaga, and H. Jónsson, J. Chem. Phys. **113**, 9901 (2000).
[33] N. Liu, L. Fu, B. Y. Dai, K. Yan, X. Liu, R. Q. Zhao, Y. F. Zhang, and Z. F. Liu, Nano Lett. **11**, 297 (2011).
[34] E. Voloshina and Y. Dedkov, Phys. Chem. Chem. Phys. **14**, 13502 (2012).
[35] P. Wu, W. H. Zhang, Z. Y. Li, and J. L. Yang, Small **10**, 2136 (2014).
[36] G. Giovannetti, P. A. Khomyakov, G. Brocks, V. M. Karpan, J. van der Brink, and P. J. Kelly, Phys. Rev. Lett. **101**, 026803 (2008).
[37] M. Vanin, J. J. Mortensen, A. K. Kelkkanen, J. M. Garcia-Lastra, K. S. Thygesen, and K. W. Jacobsen, Phys. Rev. B **81**, 081408(R) (2010).
[38] I. Hamada and M. Otani, Phys. Rev. B **82**, 153412 (2010).
[39] Y. Gamo, A. Nagashima, M. Wakabayashi, M. Terai, and C. Oshima, Surf. Sci. **374**, 61 (1997).
[40] P. Lacovig, M. Pozzo, D. Alfè, P. Vilmercati, A. Baraldi, and S. Lizzit, Phys. Rev. Lett. **103**, 166101 (2009).
[41] W. Chen, H. Chen, H. P. Lan, P. Cui, T. P. Schulze, W. G. Zhu, and Z. Y. Zhang, Phys. Rev. Lett. **109**, 265507 (2012).
[42] X. Y. Zhang, Z. W. Xu, L. Hui, J. Xin, and F. Ding, J. Phys. Chem. Lett. **3**, 2822 (2012).
[43] L. Liu *et al.*, DOI: 10.1073/pnas.1405613111 [Proc. Natl. Acad. Sci. U.S.A. (to be published)].
[44] J. Tersoff, A. W. D. van der Gon, and R. M. Tromp, Phys. Rev. Lett. **72**, 266 (1994).
[45] E. G. Seebauer and C. E. Allen, Prog. Surf. Sci. **49**, 265 (1995).
[46] J. A. Venables, G. D. T. Spiller, and M. Hanbücken, Rep. Prog. Phys. **47**, 399 (1984).
[47] X. S. Li, C. W. Magnuson, A. Venugopal, R. M. Tromp, J. B. Hannon, E. M. Vogel, L. Colombo, and R. S. Ruoff, J. Am. Chem. Soc. **133**, 2816 (2011).
[48] R. G. Van Wesep, H. Chen, W. G. Zhu, and Z. Y. Zhang, J. Chem. Phys. **134**, 171105 (2011).
[49] J. G. Amar and F. Family, Phys. Rev. B **54**, 14742 (1996).
[50] S. J. Liu, H. C. Huang, and C. H. Woo, Appl. Phys. Lett. **80**, 3295 (2002).
[51] J. Wang, H. C. Huang, S. V. Kesapragada, and D. Gall, Nano Lett. **5**, 2505 (2005).